CRACK LENGTH EFFECT ON FRACTURE BEHAVIOUR OF DUPLEX STEELS

I. Dlouhý[1], Z. Chlup[2], M. Holzmann[1]

Arising from a two-parameter fracture mechanical approach to the analysis of failure initiation condition three point bend specimens with shallow and deep cracks were tested at various temperatures. Duplex stainless steel of the type SAF 2205 has been used for analysis having microstructure after age hardening at 475°C. The effect of crack length on fracture toughness temperature diagram was analysed. Although strong dependence of measured fracture toughness on crack tip constraint was observed no evident differences in fracture morphology have been identified except for quantitative ones. Peculiarities of fracture behavior in transition and lower shelf region of DSS investigated have been explained. Fracture toughness locus (J_I-Q curve) was predicted supposing the stress controlled fracture and compared with experimental data.

INTRODUCTION

Failure of duplex stainless steels (DSS) at temperatures below ambient is characteristic by a number of peculiarities (1-4), some of them are similar to composites behaviour. Causes are seen in almost brittle nature of ferrite failure in transition region (and/or in age hardened condition) and quite different strain and fracture behaviour of ferrite and austenite. One from typical features - splitting along ferritic bands in wrought material - supposes an obstacle for exact fracture toughness measurement (2).

Welds of DSS in the offshore industry must have sufficient toughness at temperatures as low as -50°C (5). For steel applications that involve such temperatures, it is standard practice to minimise the risk of brittle fracture by imposing impact test requirements. In DSS however, there is still some uncertainty in assessment criteria as for low temperature toughness so for embrittlement due to age hardening (6).

The transferability of toughness characteristics obtained on laboratory test specimen raises the problem of geometrical and size effects. Although recent knowledge about calculation methodology of constraint indexing parameters (T-stress, Q-parameter etc. (7,8)) has contributed substantially to this problem solution, for real structural material the

[1] Institute of Physics of Materials AS CR, Žižkova 22, 61662 Brno, Czech Republic
[2] Institute of Materials Engineering, TU Brno, Technická 2, 61669 Brno, Czech Republic

more exact insight into micromechanisms of crack tip constraint phenomena is needed.

The aim of the paper can be seen in assessment of fracture micromechanisms in relation to the macroscopic fracture characteristics of DSS steel tested under two different crack tip constraint levels corresponding to different crack length. Dependence of fracture toughness on Q parameter should be also determined.

MATERIAL AND EXPERIMENTAL PROCEDURES

Material characterisation

The SAF 2205 steel used had a chemical composition (wt %): 0.025 C; 1.01 Mn; 0.31 Si; 5.40 Ni; 21.7 Cr; 3.1 Mo; 0.14 N; 0.015 P; 0.012 S. The steel was commercially produced hot rolled rod with diameter of 70 mm. Age hardened microstructure has been produced by ageing at 475 °C for 10 hrs. Selected material characteristics of as received state and microstructure investigated are shown in **Table 1**. The steel used was typical by comparable amount of ferrite and austenite crystals strongly banded in rolling direction. In the table, d_{AG} represents average austenitic grain size, d_{FG} is average ferritic grain size.

Table 1: Microstructural and selected mechanical characteristics of materials studied

state	Tempering	HV10	d_{AG} [μm]	d_{FG} [μm]	$R_p0.2$ [MPa]	R_m [MPa]	CVN impact energy [J]	DBTT [°C]
as rec		265	45x420	45x370	548	734	239	-55
aged	475°C/10hrs	301			676	805	95	+10

Mechanical testing

The tensile properties have been measured using the cylindrical specimens with diameter of 6 mm, testing was carried out at temperature ranging from -196 to +100 °C at a cross - head speed of 2 $mm.min^{-1}$. The yield strength was taken to be the 0.2 % proof stress.

Fracture toughness was tested using two test specimen types. The first one was the standard three-point bend specimen 25x50x220 mm^3 (9). The other specimen geometry was so selected to obtain the shallow crack (to a value of a/w about 0.22) and the comparable ligament area under the crack tip. In these specimens the crack was introduced under condition close to standard geometry, then the specimens were cut and grounded to final dimensions of 25x30x120 mm^3 (10). Both specimen types have been tested at 1mm/min cross-head speed over temperature range from -198 °C to +50 °C.

Charpy type (CVN) specimens loaded statically in three point bending were used for determination of critical fracture stress. At selected temperature (-180 °C) below temperature t_{gy}, at which coincidence of fracture force, F_{fr}, and general yield force, F_{gy}, occurs on their temperature dependencies, a range of bend tests was performed.

Calculations

For CVN specimen tested statically at temperature below t_{gy} the principal stress distributions below the notch were calculated. A 2D model under plane strain conditions was used for the elastic-plastic analysis using symmetry of three-point bending of V-notched specimen (11). Finite elements package ANSYS 5.1 was used for calculations.

RESULTS AND DISCUSSION

Fracture toughness temperature diagram

The temperature dependence of fracture toughness (FTTD) determined on specimens with standard crack length (a/w ~ 0.5) is shown in **Fig. 1**. A set of specimens was tested at one temperature (-120 °C) for purposes of toughness scatter assessment. Load deflection traces are typical by pop-in behaviour. Due to austenite plasticity at crack tip even at very low temperature only some specimen kept condition of LEFM for standard K_{IC} toughness values and K_C values have been obtained in lower shelf regime. In the transition and close to the upper shelf region the fracture behaviour has been characterised by K_{JC} values determined for specimen without detectable ductile tearing before fracture and K_{JU} for specimen with ductile crack extension preceding the unstable brittle fracture. $K_{J0.2}$ represents here the value for specimen with 0.2 mm ductile crack extension.

For specimens with shallow cracks (a/w ~ 0.22) the fracture toughness temperature diagram is shown in **Fig. 2**. The main characteristics of standard specimen are also depicted in the diagram by dashed lines. The shift of transition region to lower temperatures can be observed for shallow crack (lower constraint). The mean fracture toughness obtained at one test temperature (the same initiation mechanism was proved by SEM for all specimens) is higher for short crack length when compared with standard crack length. The larger scatter in fracture toughness values can be observed for shorter cracks being strongly influenced by larger crack tip plastic zone and due to this higher probability of secondary crack formation in specimens having shallow cracks. The occurrence of crack deflection due to secondary cracks (splitting in direction of ferritic bands) was observed in much more extend than in standard specimen.

Brittle fracture behaviour in lower shelf region

Duplex microstructure with nearly comparable amount of both microstructure constituents and contemporary effect of low temperature embrittlement and embrittlement due to ferrite age hardening yield to a number of peculiarities in fracture behaviour (10).

The DSS steel investigated is especially tough even in embrittled condition. Fracture takes place in several steps. First, cleavage cracks are initiated in ferrite. These cleavage cracks cross ferrite and stop at the interface with austenite. These cleavage cracks propagate into neighbouring ferrite grains and cause fracture across the whole ferrite layer (secondary cracks perpendicular to fracture surface). Nevertheless, only the grains having a favourable orientation will lead to cleavage cracks in ferrite. After this stage, cracks subsequently grow by plastic deformation of austenite. From thin foils cut from stopped tensile test was evident that the plastic deformation of austenite contributes much more to the local stress in ferrite than the applied macroscopic stress.

According to these observations, supported by results obtained on other investigated duplex steels (1-3), fracture criteria based either on critical shear stress (12,2) or critical tensile stress (4) could be applied. Almost brittle appearance of fracture surfaces at specimens broken in lower shelf region can give raise to an opinion that the fracture initiation in studied DSS may be controlled by critical tensile stress criterion although some amount of local deformation preceding the cleavage nucleation was necessary.

Temperature dependence of characteristic forces determined using statically loaded CVN specimens has been applied for critical fracture stress estimation. Data obtained on this specimen set are shown in **Fig. 3**. The general yield force at temperature t_{gy} = -165 °C reaches the value of 22.9 kN. From this value the critical fracture stress, σ_F, on level of 2449 MPa was obtained using procedure described for similar duplex steel in (4).

Principal stress distributions below notch root calculated for CVN specimen tested at -180 °C (**Fig. 4**) show values being quite comparable to critical fracture stress obtained.

J_I-Q curve - Fracture toughness locus

The fracture toughness data for specimen with standard and shallow crack tested at one temperature (-120 °C, having the same fracture micromechanism) are introduced in **Fig. 5**. The value of Q - parameter has been selected as parameter representing the crack tip constraint. For individual test specimen, the following simplified procedure of the Q-parameter calculation has been applied: For known ratio a/w the value of geometrical factor β has been determined from diagram of β on a/w (for DSS investigated shown in (12)) and T – stress has been calculated according to equation in (13)

$$T = \beta \cdot \frac{K}{\sqrt{\pi \cdot a}},$$

where β is geometrical factor, K - stress intensity factor, and a – is crack length. From known values of T-stress the Q-parameter have been determined for Ramberg - Osgood strain hardening coefficient N = 5 from dependence introduced by Shih (7).

Strong dependence of toughness values on crack tip constraint indexing parameter is obvious from Fig. 5. Shih and O´Dowd (7) suggested procedure for prediction of the triaxility effects on fracture toughness. Their approach is raising from using J_I – Q field in conjunction with a fracture criterion based on the attainment of critical stress σ_{CF} at characteristic distance X_0 (RKR model). Resulting expression is in a form

$$J_C = J_{IC} \cdot \left(1 - \frac{Q \cdot \sigma_0}{\sigma_{CF}}\right)^{(N+1)},$$

where J_C is a fracture toughness for given value of Q - parameter and J_{IC} is a fracture toughness for Q = 0 (i.e. for standard crack length). The curve in **Fig. 5** shows the variation of J_C with Q for critical fracture stress σ_{CF} = 2449 MPa, yield strength σ_0 = 929 MPa, and Ramberg - Osgood strain hardening coefficient N = 5. The exact calculation of Q-parameter is a matter of running investigations. The predicted curve appears to be in good conformity with experimental data.

CONCLUDING REMARKS

Strong dependence of measured fracture toughness values on crack length used in bend specimen was observed. This dependence was supported by predicted J_I-Q curve (fracture toughness locus) supposing the fracture initiation is controlled by critical tensile stress. Discrepancy has been found when assessing steel fracture behaviour by means of CVN specimens and precracked bend ones showing that the crack tip triaxiality plays an

important role in DSS. These steels and similar materials with specific fracture behaviour have to be accepted as special group of in situ (natural) composites.

ACKNOWLEDGMENTS

The research was financially supported by grant Nr. A 2041701 of the Grant Agency of the Academy of Sciences.

REFERENCES

(1) Kolednik, O. et al., Acta Metall. Mater., V. 44, N. 8, 1996, p. 3307;
(2) Marrow, J.T., et al., Fatig. Fract. Engng. Mat. Struct. V. 29, 1997, N. 7, p. 1005;
(3) Joly, P., Pineau, A., Scandinavian Journal of Metallurgy, 1995, V. 24, p. 226;
(4) Dlouhý, I. et al., In Proc. of 11th ECF, Poitiers, 1996, p. 651;
(5) Liljas, M., Proc. of Conf. on Duplex Stainless Steels, Glassgow, 1994, p. KV;
(6) Mockler, C. J., et al, Proc. of I.C. on DSS, Glasgow, 1994, TWI, Vol. 1, p.52;
(7) Shih, C. F., O'Dowd, N. P., In "Shallow Crack Fract. Mechan. Toughness Tests and Applications", Cambridge, Intern. Conf., TWI, Abington Publis. (1992), Paper 3;
(8) Betegon, C., Belzunce, F.J., Rodriguez, C., Acta Mater. V. 44, 1996, N. 3, pp. 1055;
(9) Unified method of test for the determination of quasistatic fracture toughens, Draft, International Standard ISO/TC164/SC4-N140, June 1996;
(10) Dlouhý, I., Chlup, Z., Holzmann, M, In: Fractography'97, p.247
(11) Kozák, V., Dlouhý, I., Holzman, M., Trans. of 14th I.C. SMiRT, Lyon, 1977, p. 681;
(12) Marrow, J.T., Fatig and Fract. Engn. Mater. Struct. Vol. 19, N. 7, 1996, pp. 935;
(13) Leevers, P.T., Radon, J.C.: Interm. J. Fract., 9 ,1982, p.311;
(14) Chlup, Z., Dlouhý, I., Metalic Mater., 1998, in print.

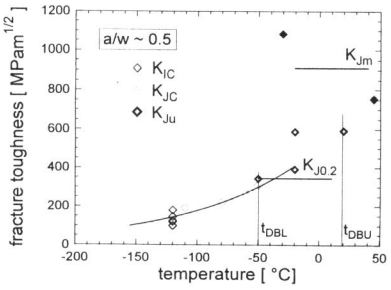

Figure 1. Temperature dependencies of fracture toughness for specimens with standard crack length

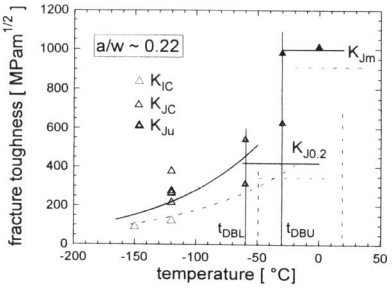

Figure 2. Temperature dependencies of fracture toughness for specimen with shallow cracks

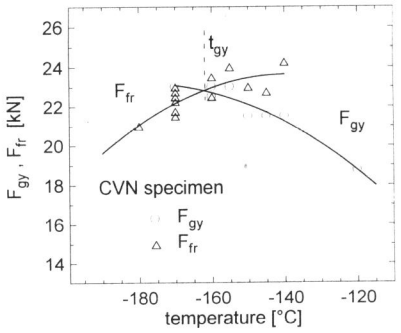

Figure 3. Temperature dependencies of fracture force and general yield force for CVN specimen

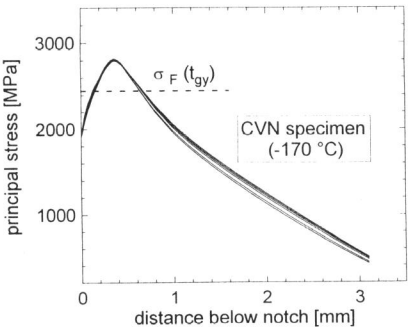

Figure 4. Principal stress distribution below notch root (left) at fracture and critical fracture stress level

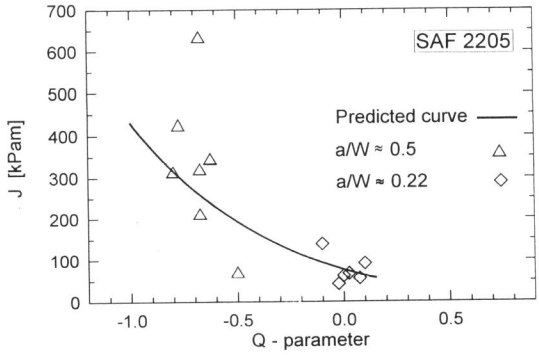

Figure 5. Dependence of experimental and predicted fracture toughness values on Q parameter